Synthesis, Characterization, and Metal Coordinating Ability of Multifunctional Carbohydrate−Containing Compounds for Alzheimer's Therapy

ARTICLE *in* JOURNAL OF THE AMERICAN CHEMICAL SOCIETY · JULY 2007

Impact Factor: 12.11 · DOI: 10.1021/ja068965r · Source: PubMed

10 AUTHORS, INCLUDING:

Tim Storr
Simon Fraser University
60 PUBLICATIONS **1,381** CITATIONS
SEE PROFILE

David E Green
University Health Network
20 PUBLICATIONS **522** CITATIONS
SEE PROFILE

Chris Orvig
University of British Columbia - Vancouver
262 PUBLICATIONS **9,416** CITATIONS
SEE PROFILE

J|A|C|S
ARTICLES
Published on Web 05/19/2007

Synthesis, Characterization, and Metal Coordinating Ability of Multifunctional Carbohydrate-Containing Compounds for Alzheimer's Therapy

Tim Storr,[†] Michael Merkel,[†] George X. Song-Zhao,[†] Lauren E. Scott,[†] David E. Green,[†] Meryn L. Bowen,[†] Katherine H. Thompson,[†] Brian O. Patrick,[†] Harvey J. Schugar,*[,‡] and Chris Orvig*[,†]

Contribution from the Medicinal Inorganic Chemistry Group, Department of Chemistry, University of British Columbia, 2036 Main Mall, Vancouver, British Columbia, V6T 1Z1, Canada and Department of Chemistry and Chemical Biology, Rutgers, The State University of New Jersey, 610 Taylor Road, Piscataway, New Jersey 08854-8087

Received December 31, 2006; E-mail: orvig@chem.ubc.ca, schugar@rutchem.rutgers.edu

Abstract: Dysfunctional interactions of metal ions, especially Cu, Zn, and Fe, with the amyloid-β (Aβ) peptide are hypothesized to play an important role in the etiology of Alzheimer's disease (AD). In addition to direct effects on Aβ aggregation, both Cu and Fe catalyze the generation of reactive oxygen species (ROS) in the brain further contributing to neurodegeneration. Disruption of these aberrant metal−peptide interactions via chelation therapy holds considerable promise as a therapeutic strategy to combat this presently incurable disease. To this end, we developed two multifunctional carbohydrate-containing compounds *N,N′*-bis[(5-β-D-glucopyranosyloxy-2-hydroxy)benzyl]-*N,N′*-dimethyl-ethane-1,2-diamine (**H_2GL^1**) and *N,N′*-bis[(5-β-D-glucopyranosyloxy-3-*tert*-butyl-2-hydroxy)benzyl]-*N,N′*-dimethyl-ethane-1,2-diamine (**H_2GL^2**) for brain-directed metal chelation and redistribution. Acidity constants were determined by potentiometry aided by UV−vis and ^{1}H NMR measurements to identify the protonation sites of **$H_2GL^{1,2}$**. Intramolecular H bonding between the amine nitrogen atoms and the H atoms of the hydroxyl groups was determined to have an important stabilizing effect in solution for the **H_2GL^1** and **H_2GL^2** species. Both **H_2GL^1** and **H_2GL^2** were found to have significant antioxidant capacity on the basis of an in vitro antioxidant assay. The neutral metal complexes **$CuGL^1$**, **$NiGL^1$**, **$CuGL^2$**, and **$NiGL^2$** were synthesized and fully characterized. A square-planar arrangement of the tetradentate ligand around **$CuGL^2$** and **$NiGL^2$** was determined by X-ray crystallography with the sugar moieties remaining pendant. The coordination properties of **$H_2GL^{1,2}$** were also investigated by potentiometry, and as expected, both ligands displayed a higher affinity for Cu^{2+} over Zn^{2+} with **H_2GL^1** displaying better coordinating ability at physiological pH. Both **H_2GL^1** and **H_2GL^2** were found to reduce Zn^{2+}- and Cu^{2+}- induced Aβ_{1-40} aggregation in vitro, further demonstrating the potential of these multifunctional agents as AD therapeutics.

Introduction

Alzheimer's disease (AD) currently affects approximately 2% of the population in North America with a predicted 3-fold increase in incidence over the next 50 years.[1] Neurodegenerative diseases, such as AD, Parkinson's disease (PD), Creutzfeldt Jakob disease (CJD), and amyotrophic lateral sclerosis (ALS), are all defined by the progressive loss of neuronal cell populations, protein aggregation, and extensive evidence of oxidative stress.[2,3] The amyloid hypothesis has long been the dominant theory to explain the etiology of AD,[4] linking the 39−42 residue amyloid-β (Aβ) peptide to the neurodegeneration in the disease. More specifically, the amyloid hypothesis postulates that plaque Aβ depositions, or partially aggregated soluble Aβ, trigger a neurotoxic cascade resulting in AD pathology.[5]

Amyloid plaques have been described as "metallic sinks" because remarkably high concentrations of Cu, Fe, and Zn have been found within these deposits in AD brains.[6,7] Cu, Fe, and Zn are increased from 3 to 5 times in AD brains as compared to those in age-matched controls.[7] Fenton-type processes involving redox-active metal ions,[8] possibly in concert with impaired

[†] University of British Columbia.
[‡] Rutgers University.

(1) www.alz.org, 10/13/06; www.alzheimer.ca, 10/13/06.
(2) Barnham, K. J.; Masters, C. L.; Bush, A. I. *Nat. Rev. Drug Discov.* **2004**, *3*, 205.
(3) (a) Doraiswamy, P. M.; Finefrock, A. E. *Lancet Neurol.* **2004**, *3*, 431. (b) Binolfi, A.; Rasia, R. M.; Bertoncini, C. W.; Ceolin, M.; Zweckstetter, M.; Griesinger, C.; Jovin, T. M.; Fernandez, C. O. *J. Am. Chem. Soc.* **2006**, *128*, 9893.
(4) (a) Hardy, J.; Selkoe, D. J. *Science* **2002**, *297*, 353. (b) Hardy, J. A.; Higgins, G. A. *Science* **1992**, *256*, 184.
(5) Selkoe, D. J. *Physiol. Rev.* **2001**, *81*, 741.
(6) Smith, M. A.; Harris, P. L. R.; Sayre, L. M.; Perry, G. *Proc. Natl. Acad. Sci. U.S.A.* **1997**, *94*, 9866.
(7) Lovell, M. A.; Robertson, J. D.; Teesdale, W. J.; Campbell, J. L.; Markesbery, W. R. *J. Neurol. Sci.* **1998**, *158*, 47.
(8) (a) Hensley, K.; Floyd, R. A. *Arch. Biochem. Biophys.* **2002**, *397*, 377. (b) Halliwell, B.; Gutteridge, J. M. *Biochem. J.* **1984**, *219*, 1. (c) Frederickson, C. J.; Koh, J. Y.; Bush, A. I. *Nat. Rev. Neurosci.* **2005**, *6*, 449. (d) Gaggelli, E.; Kozlowski, H.; Valensin, D.; Valensin, G. *Chem. Rev.* **2006**, *106*, 1995. (e) Stadtman, E. R. *Free Radical Biol. Med.* **1990**, *9*, 315. (f) Bush, A. I. *Trends Neurosci.* **2003**, *26*, 207.

Chart 1. Structures of Metal-Ion Chelators Showing Promise as AD Therapeutics

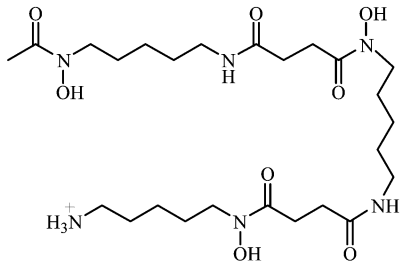

DFO

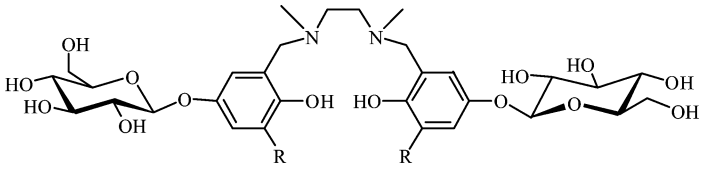

H_2GL^1 R = H
H_2GL^2 R = t-butyl

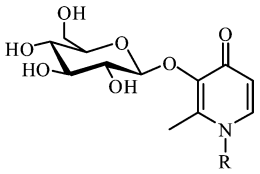

Pyridinone-conjugates

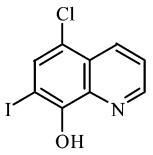

Clioquinol

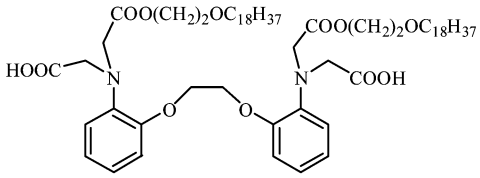

DP-109

cellular energy metabolism, lead to increased oxidative stress, a major feature of age-related neurodegenerative diseases. The interaction of Aβ with metal ions in vitro leads to aggregation with Zn^{2+} accelerating the deposition process more rapidly compared to Cu^{2+} and Fe^{3+} at pH 7.4.[9] Cu^{2+}-induced Aβ aggregation is, however, exaggerated under slightly acidic conditions (pH 6.8), and altered H^+ homeostasis (cerebral acidosis) is hypothesized to occur in AD.[10,11] Metal ions have also been shown to modify the Aβ peptide via cross-linking[12] and oxidation.[2,13] Further in vitro studies have demonstrated that Cu^{2+} and Fe^{3+} potentiate the neurotoxicity of Aβ via redox cycling and production of H_2O_2 in the presence of dioxygen.[14,15] Zn and Cu have been found to co-purify with Aβ from AD brain tissue, unlike Fe.[16] Fe in plaques is most likely involved in neuritic processes (for example, complexed to ferritin[17]) and thus may not directly interact with Aβ. However, oxygen-mediated production of ROS is often associated with increased labile Fe stores,[7] and Fe in human amyloid deposits has, in fact, been shown to be redox active.[6] Surprisingly, a recent in vitro study highlighted the potential role of Fe in blocking Cu-mediated neurotoxicity.[18] The extensive evidence of disrupted iron metabolism in AD still leaves many unanswered questions about the role of this particular metal ion in the disease.[19]

The mounting evidence supporting the role(s) of metal ions in the pathophysiology of AD has rendered metal-ion chelation therapy a promising treatment strategy. Appropriate chelators can be designed to potentially minimize oxidative stress as well as disrupt Aβ pathology. In vitro studies have shown that production of H_2O_2 via interaction of Cu^{2+} and Fe^{3+} with $A\beta_{1-42}$ is significantly attenuated by the presence of the chelators diethylenetriaminepentaacetic acid (DTPA), triethylenetetraamine (TETA), and desferrioxamine (DFO, Chart 1).[14] Treatment of the Tg2576 transgenic mouse (model for AD) with clioquinol (Chart 1), an 8-hydroxyquinoline chelator, reduced brain amyloid accumulation,[20] and the effect was recently reproduced with the lipophilic chelator DP-109 (Chart 1).[21] An early clinical study with the strong metal-ion chelator DFO showed a significant decrease in the rate of decline of treated subjects compared with the control group over a 24-month period.[22] Clioquinol has also shown indications of slowing neurological decline in early-stage clinical trials.[23] Although metal chelating agents may represent a promising therapeutic strategy, long-term use of strong chelators that are not tissue specific, such as DFO, likely affects the homeostasis of numerous biometals and the normal physiological functions of essential metal-requiring biomolecules such as metalloenzymes.[24] Specific, rather than systemic, chelation of excess metals in the brain of AD patients is therefore highly preferred. Ligands with intermediate affinity may be well suited to this

(9) Bush, A. I.; Pettingell, W. H.; Multhaup, G.; Paradis, M. d.; Vonsattel, J.-P.; Gusella, J. F.; Beyreuther, K.; Masters, C. L.; Tanzi, R. E. *Science* **1994**, *265*, 1464.
(10) Atwood, C. S.; Moir, R. D.; Huang, X.; Scarpa, R. C.; Bacarra, N. M.; Romano, D. M.; Hartshorn, M. A.; Tanzi, R. E.; Bush, A. I. *J. Biol. Chem.* **1998**, *273*, 12817.
(11) Yates, C. M.; Butterworth, J.; Tennant, M. C.; Gordon, A. *J. Neurochem.* **1990**, *55*, 1624.
(12) (a) Barnham, K. J.; Haeffner, F.; Ciccotosto, G. D.; Curtain, C. C.; Tew, D.; Mavros, C.; Beyreuther, K.; Carrington, D.; Masters, C. L.; Cherny, R. A.; Cappai, R.; Bush, A. I. *FASEB J.* **2004**, *18*. (b) Atwood, C. S.; Perry, G.; Zeng, H.; Kato, Y.; Jones, W. D.; Ling, K. Q.; Huang, X. D.; Moir, R. D.; Wang, D. D.; Sayre, L. M.; Smith, M. A.; Chen, S. G.; Bush, A. I. *Biochemistry* **2004**, *43*, 560.
(13) Barnham, K. J. et al. *J. Biol. Chem.* **2003**, *278*, 42959.
(14) Huang, X.; Atwood, C. S.; Hartshorn, M. A.; Multhaup, G.; Goldstein, L. E.; Scarpa, R. C.; Cuajungco, M. P.; Gray, D. N.; Lim, J.; Moir, R. D.; Tanzi, R. E.; Bush, A. I. *Biochemistry* **1999**, *38*, 7609.
(15) (a) da Silva, G. F. Z.; Tay, W. M.; Ming, L. J. *J. Biol. Chem.* **2005**, *280*, 16601. (b) Huang, X. et al. A. I. *J. Biol. Chem.* **1999**, *274*, 37111.
(16) Opazo, C.; Huang, X. D.; Cherny, R. A.; Moir, R. D.; Roher, A. E.; White, A. R.; Cappai, R.; Masters, C. L.; Tanzi, R. E.; Inestrosa, N. C.; Bush, A. I. *J. Biol. Chem.* **2002**, *277*, 40302.
(17) Grundkeiqbal, I.; Fleming, J.; Tung, Y. C.; Lassmann, H.; Iqbal, K.; Joshi, J. G. *Acta Neuropathol.* **1990**, *81*, 105.
(18) White, A. R.; Barnham, K. J.; Huang, X.; Voltakis, I.; Beyreuther, K.; Masters, C. L.; Cherny, R. A.; Bush, A. I.; Cappai, R. *J. Biol. Inorg. Chem.* **2004**, *9*, 269.
(19) Bishop, G. M.; Robinson, S. R.; Liu, Q.; Perry, G.; Atwood, C. S.; Smith, M. A. *Dev. Neurosci.* **2002**, *24*, 184.
(20) Cherny, R. A. et al. *Neuron* **2001**, *30*, 665.
(21) Lee, J. Y.; Friedman, J. E.; Angel, I.; Kozak, A.; Koh, J. Y. *Neurobiol. Aging* **2004**, *25*, 1315.
(22) Crapper McLachlan, D. R.; Dalton, A. J.; Kruck, T. P.; Bell, M. Y.; Smith, W. L.; Kalow, W.; Andrews, D. F. *Lancet* **1991**, *337*, 1304.
(23) (a) Regland, B.; Lehmann, W.; Abedini, I.; Blennow, K.; Jonsson, M.; Karlsson, I.; Sjogren, M.; Wallin, A.; Xilinas, M.; Gottfries, C. G. *Dement. Geriatr. Cogn. Disord.* **2001**, *12*, 408. (b) Ritchie, C. W. et al. *Arch. Neurol.* **2003**, *60*, 1685.
(24) (a) Singh, S.; Khodr, H.; Taylor, M. I.; Hider, R. C. In *Free Radicals and Oxidative Stress: Environment, Drugs and Food Additives*; Rice-Evans, C., Halliwell, B., Lunt, G. G., Eds.; Portland Press: London, 1995; pp 127. (b) Porter, J. B.; Huens, E. R. *Bailliere's Clin. Haematol.* **1989**, *2*, 459.

role; they would be capable of disrupting low affinity but pathologically relevant metal−peptide interactions.

There is considerable promise in enhancing the targeting and efficacy of metal chelators through ligand design.[25] Reports of chelators with additional antioxidant properties,[26] Aβ peptide intercalation ability,[27] and amyloid binding properties[28] are interesting developments in the field of AD therapeutics. The design of a pro-chelator, triggered by H_2O_2, was recently shown to inhibit Fe-promoted OH• radical formation, a significant advance in the design of selective metal passivating agents.[29] In this work we report the synthesis and preliminary evaluation of two carbohydrate-containing metal-ion chelators **$H_2GL^{1,2}$** (Chart 1).

Linking of carbohydrates to drug molecules, forming new derivatives and/or pro-drugs, offers the potential to increase water solubility, minimize toxicity, and improve targeting. The brain requires a significant amount of glucose to maintain normal bodily functions (up to 30% of total body glucose consumption[30]), and this demand is met by the high density of hexose transporters (GLUTs)[31] at the blood brain barrier (BBB). The GLUTs, including GLUT1, at the BBB also offer the potential for transporter-facilitated drug delivery[31] for increased brain access to drug molecules. The substrate specificity of GLUT-1 may limit the brain uptake of **$H_2GL^{1,2}$** by this approach; however, less selective glucose transporters, including GLUT-3 and GLUT-4, have been identified on BBB endothelial cells. A recent report of a series of hydroxypyridinone glycoconjugate (Chart 1) pro-ligands that, once enzymatically deprotected, act as selective, tissue-dependent metal binders, as well as ROS scavengers, is an intriguing development in AD therapy.[32] This glycoconjugate approach has been used in an effort to enhance the central nervous system (CNS) targeting of anticonvulsants,[33] analgesics,[34] dopamine derivatives,[35] anti-cancer agents,[36] and HIV therapies.[37] Positive brain uptake by a radiolabeled hydroxypyridinone glycoconjugate[32] highlights the potential of facilitated carbohydrate transport across the BBB.

Tetrahydrosalen compounds were investigated as chelators in this work as the tetradentate N_2O_2 donor set is known to have a strong affinity for metal ions,[38,39] stronger than for the hydroxypyridinone class of chelators.[32,40] In addition, the phenolic moieties of **$H_2GL^{1,2}$** have the potential to act as antioxidants.[41−43] Antioxidant molecules such as vitamin E and nonsteriodal anti-inflammatory drugs (NSAIDs) have been found to slow neurological decline in AD trials.[44] The development of multifunctional metal-ion chelating antioxidant molecules with attached carbohydrate moieties offers an attractive strategy for Alzheimer's treatment.

Experimental Section

General Methods. All solvents and chemicals (Fisher, Aldrich) were reagent grade and used without further purification unless otherwise specified. Water was deionized, purified (Barnstead D9802 and D9804 cartridges), and distilled with a Corning MP-1 Mega-Pure Still. DCl and NaOD were purchased from Cambridge Isotope Laboratories. Atomic absorption standards $Cu(NO_3)_2$ and $ZnCl_2$ were purchased from Aldrich and used directly in the potentiometry experiments. The Aβ_{1-40} peptide was purchased from Advanced ChemTech (Louisville, KY). ^{1}H and ^{13}C{^{1}H} NMR spectra were recorded on a Bruker AV-300 or AV-400 instrument at 300.13 (75.48 for ^{13}C NMR) or 400.13 (100.62 for ^{13}C NMR) MHz, respectively. Mass spectra (positive ion) were obtained on a Kratos Concept II H32Q instrument (Cs^+, LSIMS), a Macromass LCT (electrospray ionization) instrument, or a Bruker Biflex IV (MALDI) instrument. C, H, and N analyses were performed at UBC by M. Lakha (Carlo Erba analytical instrumentation). Room-temperature (293 K) magnetic susceptibilities were measured on a Johnson Matthey balance using $Hg[Co(NCS)_4]$ as the susceptibility standard; diamagnetic corrections were estimated using Pascal's constants.[45] Frozen solution X-band EPR spectra were recorded on a Bruker ECS-106 EPR spectrometer in 4-mm diameter quartz tubes. The temperature (∼130 K) was maintained by liquid nitrogen flowing through a cryostat in conjunction with a Eurotherm B-VT-2000 variable-temperature controller. The microwave frequency and magnetic field were calibrated with an EIP 625A microwave frequency counter and a Varian E500 gaussmeter, respectively. Computer simulations of the EPR spectra were performed using the XSophe-Sophe-XeprView simulation software suite.[46] UV−vis spectra were recorded using a Hewlett-Packard 8543 diode array spectrometer.

(25) Storr, T.; Thompson, K. H.; Orvig, C. *Chem. Soc. Rev.* **2006**, *35*, 534.
(26) (a) Bebbington, D.; Monck, N. J. T.; Gaur, S.; Palmer, A. M.; Benwell, K.; Harvey, V.; Malcolm, C. S.; Porter, R. H. P. *J. Med. Chem.* **2000**, *43*, 2779. (b) Ji, H. F.; Zhang, H. Y. *Bioorg. Med. Chem. Lett.* **2005**, *15*, 1257.
(27) Cherny, R. A.; Barnham, K. J.; Lynch, T.; Volitakis, I.; Li, Q. X.; McLean, C. A.; Multhaup, G.; Beyreuher, K.; Tanzi, R. E.; Masters, C. L.; Bush, A. I. *J. Struct. Biol.* **2000**, *130*, 209.
(28) Dedeoglu, A.; Cormier, K.; Payton, S.; Tseitlin, K. A.; Kremsky, J. N.; Lai, L.; Li, X. H.; Moir, R. D.; Tanzi, R. E.; Bush, A. I.; Kowall, N. W.; Rogers, J. T.; Huang, X. D. *Exp. Gerontol.* **2004**, *39*, 1641.
(29) Charkoudian, L. K.; Pham, D. M.; Franz, K. J. *J. Am. Chem. Soc.* **2006**, *128*, 12424.
(30) La Manna, J. C.; Harik, S. I. *Brain Res.* **1985**, *326*, 299.
(31) Qutub, A. A.; Hunt, C. A. *Brain Res. Rev.* **2005**, *49*, 595.
(32) Schugar, H.; Green, D. E.; Bowen, M. L.; Scott, L. E.; Storr, T.; Bohmerle, K.; Thomas, F.; Allen, D. D.; Lockman, P. R.; Merkel, M.; Thompson, K. H.; Orvig, C. *Angew. Chem., Int. Ed.* **2007**, *46*, 1716−1718; *Angew. Chem.* **2007**, *119*, 1746−1748.
(33) Battaglia, G.; La Russa, M.; Bruno, V.; Arenare, L.; Ippolito, R.; Copani, A.; Bonina, F.; Nicoletti, F. *Brain Res.* **2000**, *860*, 149.
(34) Bilsky, E. J.; Egleton, R. D.; Mitchell, S. A.; Palian, M. M.; Davis, P.; Huber, J. D.; Jones, H.; Yamamura, H. I.; Janders, J.; Davis, T. P.; Porreca, F.; Hruby, V. J.; Polt, R. *J. Med. Chem.* **2000**, *43*, 2586.
(35) (a) Fernandez, C.; Nieto, O.; Rivas, E.; Montenegro, G.; Fontenla, J. A.; Fernandez-Mayoralas, A. *Carbohydr. Res.* **2000**, *327*, 353. (b) Bonina, F.; Puglia, C.; Rimoli, M. G.; Melisi, D.; Boatto, G.; Nieddu, M.; Calignano, A.; La Rana, G.; De Caprariis, P. *J. Drug Targeting* **2003**, *11*, 25.
(36) (a) Halmos, T.; Santarromana, M.; Antonakis, K.; Scherman, D. *Eur. J. Pharm.* **1996**, *318*, 477. (b) Dunsaed, C. B.; Dornish, J. M.; Aastveit, T. E.; Nesland, J. M.; Pettersen, E. O. *Anti-Cancer Drugs* **1995**, *6*, 456. (c) Zhang, M.; Zhang, Z. H.; Blessington, D.; Li, H.; Busch, T. M.; Madrak, V.; Miles, J.; Chance, B.; Glickson, J. D.; Zheng, G. *Bioconjugate Chem.* **2003**, *14*, 709. (d) Luciani, A.; Olivier, J. C.; Clement, O.; Siauve, N.; Brillet, P. Y.; Bessoud, B.; Gazeau, F.; Uchegbu, I. F.; Kahn, E.; Frija, G.; Cuenod, C. A. *Radiology* **2004**, *231*, 135.
(37) (a) Bonina, F.; Puglia, C.; Rimoli, M. G.; Avallone, L.; Abignente, E.; Boatto, G.; Nieddu, M.; Meli, R.; Amorena, M.; de Caprariis, P. *Eur. J. Pharm. Sci.* **2002**, *16*, 167. (b) Rouquayrol, M.; Gaucher, W.; Greiner, J.; Aubertin, A. M.; Vierling, P.; Guedj, R. *Carbohydr. Res.* **2001**, *336*, 161.
(38) (a) Baran, P.; Bottcher, A.; Elias, H. *Z. Naturforsch.* **1992**, *47b*, 1681. (b) Garcia-Zarracino, R.; Ramos-Quinones, J.; Hopfl, H. *J. Organomet. Chem.* **2002**, *664*, 188. (c) Bottcher, A.; Elias, H.; Eisenmann, B.; Hilms, E.; Huber, A.; Kniep, R.; Rohr, C.; Zehnder, M.; Neuburger, M.; Springborg, J. *Z. Naturforsch. B* **1994**, *49*, 1089. (d) Bottcher, A.; Elias, H.; Glerup, J.; Neuburger, M.; Olsen, C. E.; Paulus, H.; Springborg, J.; Zehnder, M. *Acta Chem. Scand.* **1994**, *48*, 967. (e) Hinshaw, C. J.; Peng, G.; Singh, R.; Spence, J. T.; Enemark, J. H.; Bruck, M.; Kristofzski, J.; Merbs, S. L.; Ortega, R. B.; Wexler, P. A. *Inorg. Chem.* **1989**, *28*, 4483. (f) Hormnirun, P.; Marshall, E. L.; Gibson, V. C.; White, A. J. P.; Williams, D. J. *J. Am. Chem. Soc.* **2004**, *126*, 2688. (g) Klement, R.; Stock, F.; Elias, H.; Paulus, H.; Pelikan, P.; Valko, M.; Mazur, M. *Polyhedron* **1999**, *18*, 3617. (h) Correia, I.; Dornyei, A.; Jakusch, T.; Avecilla, F.; Kiss, T.; Pessoa, J. C. *Eur. J. Inorg. Chem.* **2006**, 2819.
(39) Gruenwedel, W. *Inorg. Chem.* **1968**, *7*, 495.
(40) Martell, A. E.; Smith, R. M. *Critical Stability Constants*; Plenum: New York, 1974−1989; Vols. 1−6.
(41) Burton, G. W.; Ingold, K. U. *J. Am. Chem. Soc.* **1981**, *103*, 6472.
(42) Ponticelli, F.; Trendafilova, A.; Valoti, M.; Saponara, S.; Sgaragli, G. P. *Carbohydr. Res.* **2001**, *330*, 459.
(43) Valoti, M.; Sipe, H. J.; Sgaragli, G.; Mason, R. P. *Arch. Biochem. Biophys.* **1989**, *269*, 423.
(44) (a) Sano, M.; Ernesto, C.; Thomas, R. G.; Klauber, M. R.; Schafer, K.; Grundman, M.; Woodbury, P.; Growdon, J.; Cotman, D. W.; Pfeiffer, E.; Schneider, L. S.; Thal, L. J. *N. Engl. J. Med.* **1997**, *336*, 1216. (b) Veld, B. A.; Ruitenberg, A.; Hofman, A.; Launer, L. J.; van Duijn, C. M.; Stijnen, T.; Breteler, M. M. B.; Stricker, B. H. C. *N. Engl. J. Med.* **2001**, *345*, 1515.
(45) Mabbs, F. E.; Machin, D. J. *Magnetism and Transition Metal Complexes*; Chapman and Hall: London, 1961.

Synthesis. *N,N′*-Bis[(5-*β*-D-glucopyranosyloxy-2-hydroxy)benzyl]-*N,N′*-dimethyl-ethane-1,2-diamine (H_2GL^1). A solution of 4-hydroxyphenyl-*β*-D-glucopyranoside (arbutin) **1** (10.01 g, 36.8 mmol), paraformaldehyde (1.20 g, 40.00 mmol), and *N,N′*-dimethyl-1,2-ethane-diamine **2** (1.470 g, 16.68 mmol) in EtOH (150 mL) was heated to reflux for 24 h, and then the solvent was removed in vacuo. The residue was purified by silica-gel chromatography (1:1 MeOH:EtOAc eluent) to afford the product H_2GL^1 as a white solid (4.122 g, 39%). ^{1}H NMR (MeOH-d_4, 300 MHz): δ 6.96 (dd, $^4J_{b,d}$ = 2.8 Hz, $^3J_{a,b}$ = 8.7 Hz, 2H; Ar*H*), 6.90 (d, $^4J_{b,d}$ = 2.8 Hz, 2H; Ar*H*), 6.70 (d, $^3J_{a,b}$ = 8.7 Hz, 2H; Ar*H*), 4.77 (d, $^3J_{1,2}$ = 7.5 Hz, 2H; *H*-1), 3.89 (dd, $^3J_{5,6b}$ = 1.7 Hz, $^2J_{6a,6b}$ = 12.0 Hz, 2H; *H*-6b), 3.73 (dd, $^3J_{5,6a}$ = 5.4 Hz, $^2J_{6a,6b}$ = 12.0 Hz, 2H; *H*-6a), 3.68 (s, 2H; ArCH_2), 3.30−3.45 (m, 8H; *H*-2, *H*-3, *H*-4, *H*-5), 2.69 (s, 4H, NCH_2CH_2N), 2.28 (s, 6H, NCH_3). ^{13}C NMR (MeOH-d_4, 75.48 MHz): δ 153.91, 152.26 (Ar*C*), 124.50 (Ar*C*), 119.47, 118,70, 117.26 (Ar*C*H), 103.68 (*C*1), 78.12 (*C*3/*C*5), 75.14 (*C*2), 71.62 (*C*4), 62.76, 61.36 (*C*6/Ar*C*H_2), 55.03 (N*C*H_2CH_2N), 42.06 (N*C*H_3). MS (+ES-MS) *m*/*z* (relative intensity) = 657 ([L + H]$^+$, 100), 373.6 ([L − $C_{13}H_{15}O_7$]$^+$, 40). UV−vis (MeOH): λ_{max} (ϵ_{max}) = 226 nm (1.1 × 10^4 L mol^{-1} cm^{-1}), 289 nm (5.4 × 10^3 L mol^{-1} cm^{-1}). Anal. Calcd (found) for $C_{30}H_{44}N_2O_{14}\cdot H_2O$: C, 53.41 (53.65); H, 6.87 (7.12); N, 4.15 (4.03).

3-*tert*-Butyl-4-hydroxyphenyl-2,3,4,6-tetra-*O*-acetyl-*β*-D-glucopyranoside (4). The title compound was synthesized by a method different from that available in the literature.[42] *tert*-Butyl-hydroquinone **3** (0.535 g, 3.22 mmol) and pentaacetylglucose (1.05 g, 2.69 mmol) were dissolved in dry CH_2Cl_2 (30 mL), and with stirring, $BF_3\cdot OEt_2$ (1.90 g, 13.41 mmol) was added dropwise. A saturated $NaHCO_3$ (30 mL) solution was added after 4 h, and the resulting mixture was extracted with CH_2Cl_2 (2 × 30 mL). The combined organic extracts were dried over Na_2SO_4 and filtered, and then the solvent was removed in vacuo. The crude product was purified by silica-gel chromatography (1:1 then 2:1 Et_2O:pet. ether eluent) to afford the product **4** as a white solid (0.931 g, 70%). ^{1}H NMR ($CHCl_3$-d_1, 300 MHz): δ 6.94 (d, $^4J_{b,d}$ = 2.9 Hz, 1H; Ar*H*), 6.71 (dd, $^4J_{b,d}$ = 2.9 Hz, $^3J_{a,b}$ = 8.5 Hz, 1H; Ar*H*), 6.57 (d, $^3J_{a,b}$ = 8.5 Hz, 1H; Ar*H*), 5.19 (m, 3H; *H*-2, *H*-3, *H*-4), 4.96 (d, $^3J_{1,2}$ = 7.5 Hz, 1H; *H*-1), 4.73 (br. s, 1H; O*H*), 4.22 (dd, $^3J_{5,6a}$ = 5.2 Hz, $^2J_{6a,6b}$ = 12.6 Hz, 1H; *H*-6a), 4.15 (dd, $^3J_{5,6b}$ = 2.4 Hz, $^2J_{6a,6b}$ = 12.6 Hz, 1H; *H*-6b), (ddd, $^3J_{4,5}$ = 9.5 Hz, $^3J_{5,6a}$ = 5.2 Hz, $^3J_{5,6b}$ = 2.4 Hz, 2H; *H*-5), 2.08 (s, 6H; 2× COCH_3), 2.04 (s, 3H; COCH_3), 2.03 (s, 3H; COCH_3), 1.38 (s, 18H; C(CH_3)$_3$). MS (+CI-MS) *m*/*z* (relative intensity) = 514 ([L + NH_4]$^+$, 90), 331 ([L − $C_{10}H_{13}O_2$]$^+$, 100). Anal. Calcd (found) for $C_{24}H_{32}O_{11}$: C, 58.06 (57.95); H, 6.50 (6.47).

***N,N′*-Bis-(3-(5-*tert*-butyl-4-hydroxyphenyl-2,3,4,6-tetra-*O*-acetyl-*β*-D-glucopyranoside)benzyl)-*N,N′*-dimethyl-ethane-1,2-diamine (5).** A solution of **4** (3.90 g, 7.86 mmol), paraformaldehyde (0.26 g, 8.57 mmol), and *N,N′*-dimethyl-ethane-1,2-diamine **2** (0.315 g, 3.57 mmol) in dry benzene (40 mL) was stirred and heated to reflux for 22 h. The solvent was then removed in vacuo, and the residue was purified by silica-gel chromatography (3:1 Et_2O:pet. ether eluent) to afford the product **5** as a white solid (2.49 g, 63%). ^{1}H NMR ($CHCl_3$-d_1, 300 MHz): δ 10.60 (s, 2H; OH), 6.87 (d, $^4J_{b,d}$ = 2.7 Hz, 2H; ArH), 6.50 (d, $^4J_{b,d}$ = 2.7 Hz, 2H; ArH), 5.25 (m, 6H; H-2, H-3, H-4), 4.94 (d, $^3J_{1,2}$ = 7.5 Hz, 2H; H-1), 4.27 (dd, $^3J_{5,6a}$ = 5.2 Hz, $^2J_{6a,6b}$ = 12.3 Hz, 2H; H-6a), 4.15 (dd, $^3J_{5,6b}$ = 2.2 Hz, $^3J_{6a,6b}$ = 12.3 Hz, 1H; H-6b), 3.81 (ddd, $^3J_{5,6a}$ = 5.2 Hz, $^3J_{5,6b}$ = 2.2 Hz, $^3J_{4,5}$ = 9.6 Hz, 2H; H-5), 3.61 (s, 4H; ArCH_2), 2.59 (s, 4H; NCH_2CH_2N), 2.25 (s, 6H; NCH_3), 2.08 (s, 6H; COCH_3), 2.07 (s, 6H; COCH_3), 2.04 (s, 6H; COCH_3), 2.0 (s, 6H; COCH_3), 1.36 (s, 18H; C(CH_3)$_3$). MS (+LSIMS) m/z (relative intensity) = 1105 ([L + H]$^+$, 30), 552 ([L − $C_{27}H_{38}NO_{11}$]$^+$, 100). Anal. Calcd (found) for $C_{54}H_{76}N_2O_{22}$: C, 58.69 (59.11); H, 6.93 (7.07); N, 2.53 (2.69).

***N,N′*-Bis[(5-*β*-D-glucopyranosyloxy-3-*tert*-butyl-2-hydroxy)benzyl]-*N,N′*-dimethyl-ethane-1,2-diamine (H_2GL^2).** Compound **5** (5.90 g, 7.68 mmol) was dissolved in dry MeOH (100 mL), and NaOMe (1.15 g, 21.3 mmol) was added with stirring. Rexyn (H^+ form) was added after 2 h, and then the mixture was filtered and the solvent removed under reduced pressure. The crude material was purified by silica gel chromatography (4:1 EtOAc:MeOH eluent) to afford the product H_2GL^2 as a white solid (3.81 g, 93%).^{1}H NMR (MeOH-d_4, 300 MHz): δ 7.02 (d, $^4J_{b,d}$ = 2.8 Hz, 2H; Ar*H*), 6.73 (d, $^4J_{b,d}$ = 2.8 Hz, 2H; Ar*H*), 4.86 (d, $^3J_{1,2}$ = 7.5 Hz, 2H; *H*-1), 3.83 (dd, $^3J_{5,6b}$ = 1.7 Hz, $^2J_{6a,6b}$ = 12.1 Hz, 2H; *H*-6b), 3.74 (dd, $^3J_{5,6a}$ = 3.1 Hz, $^2J_{6a,6b}$ = 12.1 Hz, 2H; *H*-6a), 3.68 (s, 4H; ArCH_2), 3.44 (m, 8H; *H*-2, *H*-3, *H*-4, *H*-5), 2.66 (s, 4H, NCH_2CH_2N), 2.27 (s, 6H, NCH_3), 1.39 (s, 18H; C(CH_3)$_3$). ^{13}C NMR (MeOH-d_4, 75.48 MHz): δ 153.56, 151.84 (Ar*C*), 139.02 (Ar*C*), 124.52 (Ar*C*), 117.11, 116.93 (Ar*C*H), 104.2 (*C*1), 78.46 (*C*3/*C*5), 75.45 (*C*2), 71.96 (*C*4), 63.57, 63.08 (*C*6/ArCH_2), 54.80 (NCH_2CH_2N), 41.95 (NCH_3), 36.16 (*C*(CH_3)$_3$), 30.52 (C(CH_3)$_3$). MS (+ES-MS) *m*/*z* (relative intensity) = 791 ([L + Na]$^+$, 10), 769 ([L + H]$^+$, 100). UV−vis (MeOH): λ_{max} (ϵ_{max}) = 231 nm (1.2 × 10^4 L mol^{-1} cm^{-1}), 288 nm (6.2 × 10^3 L mol^{-1} cm^{-1}). Anal. Calcd (found) for $C_{38}H_{60}N_2O_{14}\cdot H_2O$: C, 58.00 (58.40); H, 7.94 (7.92); N, 3.56 (3.57).

$CuGL^1\cdot 2H_2O$. H_2GL^1 (0.096 g, 0.15 mmol) and $Cu(ClO_4)_2\cdot 6H_2O$ (0.054 g, 0.15 mmol) were dissolved in MeOH (5 mL), and aqueous NaOH (0.5 mL, 1 M) was added with stirring. The resulting green suspension was stirred for 2 h, and then the solvent was removed in vacuo. The residue was dissolved in a minimum amount of H_2O and purified by size-exclusion chromatography on Sephadex G-10 (H_2O eluent) to afford the product $CuGL^1\cdot 2H_2O$ as a dark green solid (0.047 g, 47%). MS (+ES-MS) *m*/*z* (relative intensity) = 720/718 ([M + H]$^+$, 100), 657 ([L + H]$^+$, 20), 557/555 ([M − $C_6H_{11}O_5$]$^+$, 50). EPR (130 K, MeOH): $A_\perp$ = 20 × 10^{-4} cm^{-1}, $g_\perp$ = 2.037, $A_\parallel$ = 179 × 10^{-4} cm^{-1}, $g_\parallel$ = 2.215. UV−vis (MeOH): λ_{max} (ϵ_{max}) = 243 nm (2.8 × 10^4 L mol^{-1} cm^{-1}), 290 nm (1.5 × 10^4 L mol^{-1} cm^{-1}), 420 nm (2.0 × 10^3 L mol^{-1} cm^{-1}), 601 nm (7.0 × 10^2 L mol^{-1} cm^{-1}). The room-temperature solid-state magnetic moment μ_{eff} = 1.74 μ_B. Anal. Calcd (found) for $C_{30}H_{42}CuN_2O_{14}\cdot 2H_2O$: C, 47.77 (47.82); H, 6.15 (5.90); N, 3.71 (3.63).

$NiGL^1\cdot 3H_2O$. A stirred solution of H_2GL^1 (0.101 g, 0.15 mmol) and $Ni(ClO_4)_2\cdot 6H_2O$ (0.055 g, 0.15 mmol) in MeOH (4 mL) turned red upon addition of NEt_3 (0.031 g, 0.31 mmol). After 12 h, addition of CH_3CN (2 mL) caused the product to separate as an oily residue. The residue was recovered by decantation and redissolved in 5 mL of H_2O The product $NiGL^1\cdot 3H_2O$ was precipitated as a red-brown solid following addition of CH_3CN (2 mL) and dried (0.027 g, 25%). MS (+ES-MS) *m*/*z* (relative intensity) = 713 ([M + H]$^+$, 100). Anal. Calcd (found) for $C_{30}H_{42}N_2NiO_{14}\cdot 3H_2O$: C, 46.95 (47.03); H, 6.30 (6.21); N, 3.65 (3.42).

$CuGL^2\cdot 2MeOH$. Aqueous NaOH (0.5 mL, 1 M) was added to a green solution of H_2GL^2 (0.082 g, 0.11 mmol) and $Cu(ClO_4)_2\cdot 6H_2O$ (0.040 g, 0.11 mmol) in MeOH (4 mL). The solution was stirred for 2 h, and then the solvent was removed in vacuo. The residue was dissolved in a minimum amount of MeOH and purified by size-exclusion chromatography on Sephadex G-10 (MeOH eluent) to afford the product $CuGL^2\cdot 2$MeOH as a dark green solid (0.050 g, 56%). MS (+ES-MS) *m*/*z* (relative intensity) = 854/852 ([M + Na]$^+$, 100), 830 ([M + H]$^+$, 10). EPR (130 K, MeOH): A_x = 24 × 10^{-4} cm^{-1}, g_x = 2.040, A_y = 30 × 10^{-4} cm^{-1}, g_y = 2.020, A_z = 178 × 10^{-4} cm^{-1}, g_z = 2.215. UV−vis (MeOH): λ_{max} (ϵ_{max}) = 247 nm (1.7 × 10^4 L mol^{-1} cm^{-1}), 297 nm (1.2 × 10^4 L mol^{-1} cm^{-1}), 445 nm (2.7 × 10^3 L mol^{-1} cm^{-1}), 620 nm (1.4 × 10^3 L mol^{-1} cm^{-1}). The room-temperature solid-state magnetic moment μ_{eff} = 1.79 μ_B. Anal. Calcd (found) for $C_{38}H_{58}CuN_2O_{14}\cdot 2$MeOH: C, 53.71 (53.38); H, 7.44 (7.30); N, 3.13 (3.23).

$NiGL^2\cdot H_2O$. Triethylamine NEt_3 (0.036 g, 0.36 mmol) was added to a stirred solution of H_2GL^2 (0.051 g, 0.07 mmol) and $Ni(ClO_4)_2\cdot 6H_2O$ (0.024 g, 0.07 mmol) in MeOH (2 mL). The color of the reaction mixture changed from light pink to dark red over a period of 24 h.

(46) (a) Wang, D. M.; Hanson, G. R. *J. Mag. Reson., Ser. A* **1995**, *117*, 1. (b) Hanson, G. R.; Gates, K. E.; Noble, C. J.; Griffin, M.; Mitchell, A.; Benson, S. *J. Inorg. Biochem.* **2004**, *98*, 903.

Table 1. Crystal Data for **H_2GL^2**, **$CuGL^2$**, and **$NiGL^2$**

cryst data	H_2GL^2	$CuGL^2$	$NiGL^2$
formula	$C_{38}H_{68}N_2O_{18.25}$	$C_{38}H_{58}CuN_2O_{14}$	$C_{42}H_{74}N_2NiO_{18}$
fw	844.95	830.40	953.74
cryst syst, space group	triclinic, *P*1 (#1)	triclinic, *P*1 (#1)	monoclinic, $P2_1$ (#4)
a (Å)	10.498 (1)	10.691 (2)	14.993 (3)
b (Å)	10.748 (1)	8.7559 (9)	9.2197 (18)
c (Å)	39.414 (3)	13.602 (2)	16.607 (3)
α (deg)	87.66 (1)	95.700 (1)	90.00
β (deg)	86.31 (1)	90.080 (1)	94.823 (7)
γ (deg)	89.89 (2)	92.050 (7)	90.00
V [Å^3]	4434.3 (8)	2349.4 (7)	2287 (7)
Z, D_{calcd} [g/cm^3]	4, 1.266	2, 1.174	2, 1.385
μ(Mo Kα) [cm^{-1}]	1.00	52.3	50.0
F_{000}	1824	882	1024
temp. (K)	173 (2)	173 (2)	173 (2)
$\theta_{min-max}$, deg	1.55, 22.49	2.16, 27.87	2.46, 21.96
reflns collcd/ unique	53 561/18 652 (R_{int} = 0.066)	20 637/15 770 (R_{int} = 0.044)	12 661/5383 (R_{int} = 0.089)
residuals (F^2, all data)	wR_2 = 0.179	wR_2 = 0.213	wR_2 = 0.189
residuals (F, $I > 2\sigma(I)$)	R_1 = 0.063	R_1 = 0.082	R_1 = 0.084

The reaction mixture was filtered, and the filtrate was left to stand for 3 days over which time red crystals of the product **$NiGL^2$**·H_2O formed. X-ray-quality crystals were isolated by decanting the supernatant liquid and washing with a minimum amount of cold MeOH to afford the crystalline product **$NiGL^2$**·H_2O (0.012 g, 20%). MS (+ES-MS) *m*/*z* (relative intensity) = 847 ([M + Na]$^+$, 60), 826 ([M + H]$^+$, 90), 792 ([L + Na]$^+$, 10), 769 ([L + H]$^+$, 100). Anal. Calcd (found) for $C_{38}H_{58}N_2NiO_{14}$·H_2O: C, 54.10 (53.86); H, 7.17 (7.18); N, 3.32 (3.42).

X-ray Crystallography. Crystals of **H_2GL^2** and **$CuGL^2$** were grown from concentrated MeOH/H_2O solutions of the respective compounds, whereas crystals of **$NiGL^2$** were obtained via slow evaporation of a concentrated MeOH solution. The crystals were mounted on a glass fiber, and measurements were made on a Bruker X8 APEX diffractometer for **H_2GL^2** and a Rigaku/ADSC CCD area detector for **$CuGL^2$** and **$NiGL^2$** with graphite-monochromated Mo Kα radiation. All data were processed and corrected for Lorentz and polarization effects and absorption using the SADABS[47] program for **H_2GL^2** and the d*TREK[48] program for **$CuGL^2$** and **$NiGL^2$**. The structures were solved by direct methods[49] and expanded using Fourier techniques.[50] A large number of disordered water and MeOH molecules were removed from the unit cell of **$CuGL^2$**, and the program PLATON/SQUEEZE[51] was used to account for the residual electron density. Final refinements were carried out using SHELXL-97[52] for **H_2GL^2** and teXsan[53] for **$CuGL^2$** and **$NiGL^2$**. The relevant parameters for crystal data, structure solution, and refinement are summarized in Table 1. CIF files are found in the Supporting Information.

Potentiometric Measurements. Equilibrium constants for protonation and complexation reactions with **$H_2GL^{1,2}$** were determined by pH-metric measurements (pH = −log [H$^+$]) in 0.16 M NaCl at 298 ± 0.1 K using a system that has been described previously.[54,55] The value of pK_w used was 13.76.[56] The glass electrode was calibrated as a hydrogen concentration probe by titrating known amounts of HCl with CO_2-free NaOH solutions and determining the equivalence point by Gran's method.[57] Acidity constants for the compounds **$H_2GL^{1,2}$** were determined by titrating 50 mL of aqueous 2.5 mM HCl in the presence of 0.6 mM **H_2GL^1** or **H_2GL^2** with 0.1 M NaOH. The constants were calculated with data in the range 4.5 ≤ pH ≤ 10.5 (for **H_2GL^1**) and 3.7 ≤ pH ≤ 10.0 (for **H_2GL^2**) using the computer program HYPERQUAD;[58,59] an average of eight independent titrations were used in determining the final values. The stability constants of Cu^{2+} and Zn^{2+} with **$H_2GL^{1,2}$** were determined by titrating a solution of 0.6 mM (Cu^{2+} or Zn^{2+}) and 0.6 mM (**H_2GL^1** or **H_2GL^2**) with 0.1 M NaOH. The stability constants were calculated using HYPERQUAD[58,59] with data in the range 4.5 ≤ pH ≤ 10.0. The acidity constants for **$H_2GL^{1,2}$** as well as the respective metal hydrolysis constants[60] were used in the stability constant calculations. The final values for the stability constants were an average of at least five independent titrations. Speciation diagrams for **$H_2GL^{1,2}$** and the M^{2+}:**$H_2GL^{1,2}$** (M = Cu^{2+}, Zn^{2+}) systems were calculated using the program HYSS.[59] pM values were calculated with a locally written Basic program for Cu^{2+} and Zn^{2+} (1 mM) and selected ligands for a ratio of 1:1 M^{2+}:ligand.

Table 2. Selected Bond Lengths (Å) in **H_2GL^2**

C(19)−C−(38)	1.53(1)	C(7)−O(1)	1.407(8)
N(1)−C(17)	1.471(8)	C(1)−O(1)	1.380(9)
N(1)−C(19)	1.469(9)	C(20)−O(8)	1.398(7)
N(2)−C(36)	1.468(8)	C(26)−O(8)	1.404(7)
N(2)−C(38)	1.462(9)		
C(10)−O(7)	1.387(8)	H bonding	
C(29)−O(14)	1.374(7)	O(7)···N(1)	2.66(1)
		O(14)···N(2)	2.68(1)

UV−vis Determination of Acidity Constants. Solutions of either **H_2GL^1** or **H_2GL^2** (0.125 mM, *I* = 0.16 M NaCl, *T* = 298 K) were prepared, the pH of each solution was adjusted, and the UV−vis spectrum was then recorded. At least 20 readings were taken in the pH range 8−13.5. Four separate experiments were carried out for each ligand, and each experiment was monitored at two different wavelengths (237 and 308 nm for **H_2GL^1**; 248 and 310 nm for **H_2GL^2**). pK_a values were calculated by fitting the absorption values and corresponding pH values using a locally written Basic program employing a Newton−Gauss nonlinear-least-squares curve-fit procedure.

Antioxidant Studies. Compounds **$H_2GL^{1,2}$** were tested for their ability to scavenge free radicals using the trolox equivalent antioxidant capacity (TEAC) assay.[61] An 2,2′-azinobis(3-ethylbenzothiazoline-6-sulfonic acid ($ABTS^{\bullet+}$) radical cation decolorization assay[61] was used to determine relative TEAC values. ABTS was dissolved in water (7 mM) and reacted with potassium persulfate (2.45 mM) in the dark for 16 h to form the colored $ABTS^{\bullet+}$ radical cation. The $ABTS^{\bullet+}$ solution was diluted with MeOH to an absorbance value of 0.70 (±0.02) at 740 nm after equilibrating to 30 °C. Solutions of **$H_2GL^{1,2}$** in MeOH (20 μL, 2.5−7.5 μM) were added to 2 mL of $ABTS^{\bullet+}$ solution to initiate the reaction. After initial mixing, $A_{740\ nm}$ was measured at 30 °C after

(47) *SADABS*, Version 2.05; Bruker AXS Inc.: Madison, WI, 1999.
(48) *d*TREK: Area Detector Software*, Version 7.11; Molecular Structure Corp., The Woodlands, TX, 2001.
(49) SIR97: Altomare, A.; Burla, M. C.; Camalli, M.; Cascarano, G. L.; Giacovazzo, C.; Guagliardi, A.; Moliterni, A. G. G.; Polidori, G.; Spagna, R. *J. Appl. Crystallogr.* **1999**, *32*, 115.
(50) DIRDIF94: Beurskens, P. T.; Admiraal, G.; Beurskens, G.; Bosman, W. P.; de Gelder, R.; Israel, R.; Smits, J. M. M. *The DIRDIF-94 program system;* Technical Report of the Crystallography Laboratory, University of Nijmegen: The Netherlands, 1994.
(51) PLATON/SQUEEZE. (a) Spek, A. L. *Acta Crystallogr.* **1990**, *A46*, C34. (b) Sluis, P. V. D.; Spek, A. L. *Acta Crystallogr.* **1990**, *A46*, 194−201. (c) Spek, A. L. *PLATON, A Multipurpose Crystallographic Tool*; Utrecht University: Utrecht, The Netherlands, 1998.
(52) *SHELXL*, Version 5.1; Bruker AXS Inc.: Madison, WI, 1997.
(53) *TeXsan: Crystal Structure Analysis Package*; Molecular Structure Corp., The Woodlands, TX, 1992.
(54) (a) Caravan, P.; Gelmini, L.; Glover, N.; Herring, F. G.; Li, H.; McNeill, J. H.; Rettig, S. J.; Setyawati, I. A.; Shuter, E.; Sun, Y.; Tracey, A. S.; Yuen, V. G.; Orvig, C. *J. Am. Chem. Soc.* **1995**, *117*, 12759. (b) Song, B.; Kurokawa, G. S.; Liu, S.; Orvig, C. *Can. J. Chem.* **2001**, *79*, 1058. (c) Song, B.; Storr, T.; Liu, S.; Orvig, C. *Inorg. Chem.* **2002**, *41*, 685.
(55) Song, B.; Mehrkhodavandi, P.; Buglyo, P.; Mikata, Y.; Shinohara, Y.; Yoneda, K.; Yano, S.; Orvig, C. *J. Chem. Soc., Dalton Trans.* **2000**, *8*, 1325.
(56) Martell, A. E.; Motekaitis, R. J. *Determination and Use of Stability Constants*; VCH: New York, 1988.
(57) Gran, G. *Analyst* **1952**, *77*, 661.
(58) Gans, P.; Sabatini, A.; Vacca, A. *Talanta* **1996**, *43*, 1739.
(59) Alderighi, L.; Gans, P.; Ienco, A.; Peters, D.; Sabatini, A.; Vacca, A. *Coord. Chem. Rev.* **1999**, *184*, 311.
(60) Baes, C. F., Jr.; Mesmer, R. E. *The Hydrolysis of Cations*; R. E. Krieger Publishing Co.: Malabar, FL, 1986.
(61) Re, R.; Pellegrini, N.; Proteggente, A.; Pannala, A.; Yang, M.; Rice-Evans, C. *Free Radical Biol. Med.* **1999**, *26*, 1231.

Scheme 1. Synthesis of **H_2GL^1** [a]

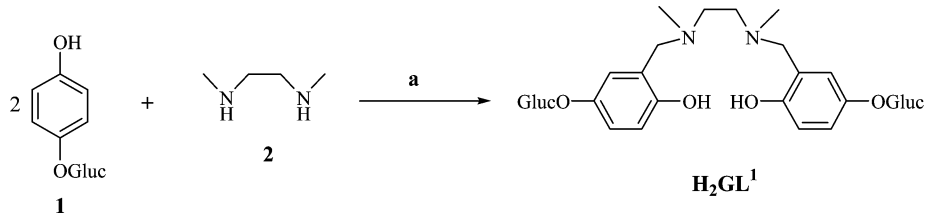

[a] (a) Paraformaldehyde, EtOH, 39%.

Scheme 2. Synthesis of **H_2GL^2** [a]

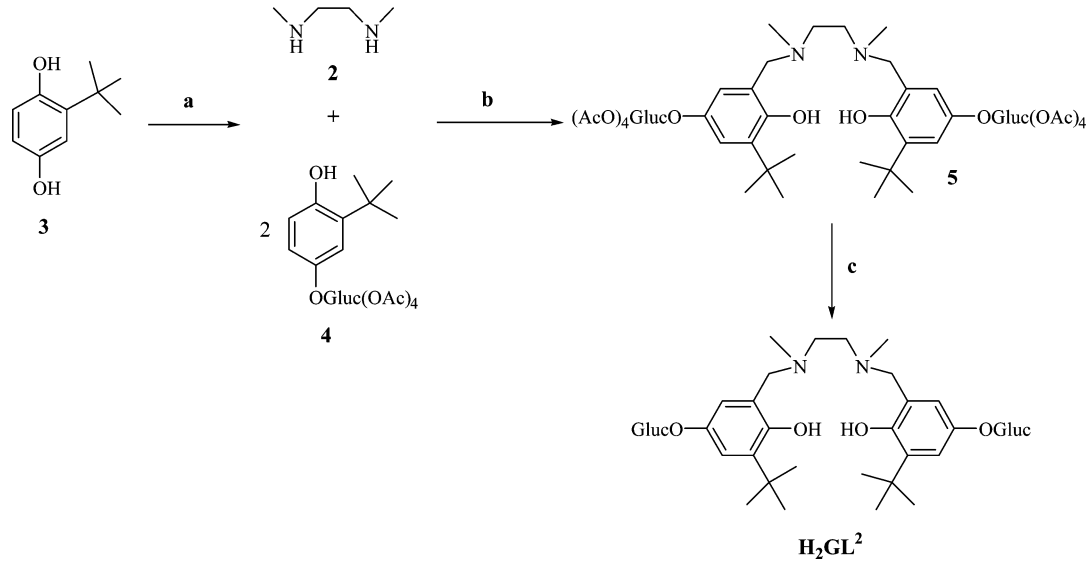

[a] (a) Pentaacetylglucose, $BF_3{\cdot}OEt_2$, CH_2Cl_2, 70%. (b) Paraformaldehyde, benzene, 63%. (c) NaOMe, MeOH, 93%.

1, 3, and 6 min, with each experiment performed in triplicate. The percentage change of the absorbance at 740 nm was calculated and plotted as a function of **$H_2GL^{1,2}$** concentration. The slopes were then compared to the standard, trolox (6-hydroxy-2,5,7,8-tetramethylchromane-2-carboxylic acid), with its TEAC value normalized to 1.

Aβ Turbidity Measurements. Lyophilized synthetic human $A\beta_{1-40}$ amyloid peptide was prepared as a ~200 μM solution in distilled, deionized water. To achieve full peptide dissolution while avoiding frothing, intermittent sonication (1 min on, 30 s off) was repeated 3 times; the solution was then filtered through a 0.2-μm syringe filter (Whatman) to remove any microparticulate protein matter. A bicinchoninic acid (BCA) assay was performed to quantify (relatively, versus bovine serum albumin, BSA) the concentration of the Aβ peptide.[62] Two Chelex-treated 4-(2-hydroxyethyl)-1-piperazineethanesulphonic acid (HEPES, 20 μM) buffer solutions containing 150 μM NaCl were prepared with distilled, deionized water to pH values of 6.6 and 7.4. These solutions were filtered through 0.22-μm acetate filters (Millipore) to remove any particulate material and used in subsequent preparations of metal, ligand, and reaction mixture solutions. Stock solutions of Cu^{2+} and Zn^{2+} were prepared from standards to final concentrations of 200 μM using pH 6.6 and 7.4 buffers, respectively. Solutions of the free ligands (DTPA, **H_2GL^1**, and **H_2GL^2**) were prepared in HEPES buffer to final concentrations of 200 μM. Turbidity assays were performed in flat-bottomed 200 μL 96-well microtiter plates (Falcon). To evaluate the effects of the test ligands, the ligand of interest (50 μM) was added after a short delay (~2 min) to a solution of the $A\beta_{1-40}$ peptide (~ 25 μM) and either Zn^{2+} (25 μM) or Cu^{2+} (25 μM). After a 45-min incubation, the 405-nm absorbances of all test solutions were measured using a Labsystems iEMS (Zn^{2+}) or Molecular Devices Thermomax (Cu^{2+}) microplate reader programmed to agitate the plate for 30 s to evenly suspend any aggregates before all readings. In all cases, appropriate blank trials were run and accounted for; wells containing Aβ peptide and the respective test ligand in HEPES buffer were used as blanks for spectrophotometric analysis. MALDI spectroscopic analysis of selected wells performed after turbidity assay exhibited peaks consistent with intact $A\beta_{1-40}$ peptide, confirming that no degradation of the peptide occurred during the assay.

Table 3. Deprotonation Constants (pK_a's) of **$H_2GL^{1,2}$** Determined by Potentiometric Measurement in 0.16 M NaCl at 298 K (errors are for the last digit)

reaction	H_2GL^1	H_2GL^2
$[HGL^{1,2}]^- \rightleftarrows [GL^{1,2}]^{2-} + H^+$ (pK_{a4})	11.3(3)[a]	13.7(5)[a]
$H_2GL^{1,2} \rightleftarrows [HGL^{1,2}]^- + H^+$ (pK_{a3})	10.30(5)[b]	13.1(5)[a]
$[H_3GL^{1,2}]^+ \rightleftarrows H_2GL^{1,2} + H^+$ (pK_{a2})	8.03(6)	6.47(4)
$[H_4GL^{1,2}]^{2+} \rightleftarrows [H_3GL^{1,2}]^+ + H^+$ (pK_{a1})	5.01(4)	4.02(9)

[a] Determined spectrophotometrically. [b] Determined by both spectrophotometric (10.2(2)) and potentiometric (10.30(5)) methods.

Results and Discussion

Synthesis and Characterization of the Carbohydrate-Appended Ligands $H_2GL^{1,2}$. The pro-ligands **H_2GL^1** and **H_2GL^2** were designed to chelate metal ions in their deprotonated forms while carrying carbohydrate moieties to enhance solubility and improve targeting ability. **H_2GL^1** was synthesized in moderate yield by the coupling of commercially available arbutin **1** with *N*,*N*′-dimethylethylenediamine via a Mannich condensation[63] (Scheme 1).

The synthesis of **H_2GL^2** is shown in Scheme 2. In the first step *tert*-butylhydroquinone **3** was glycosylated with pen-

(62) Walker, J. M., Ed. *The Protein Protocols Handbook*; 2nd ed.; Humana Press: New Jersey, 2002.

(63) Tramonti.M. *Synthesis* **1973**, 703.

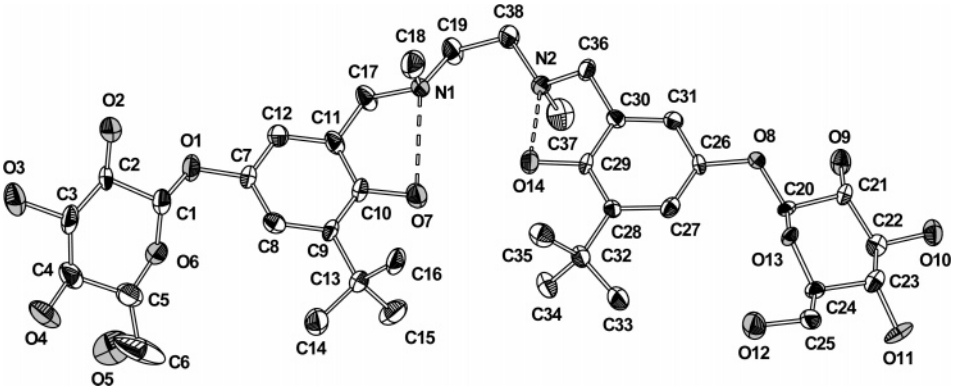

Figure 1. Ellipsoid plot (50% probability, H atoms omitted for clarity) of $\mathbf{H_2GL^2}$.

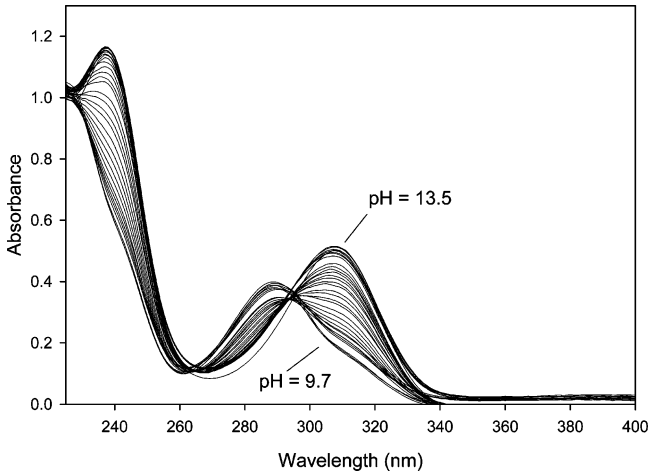

Figure 2. Variable pH (pH 9.7−13.5) UV spectra of $\mathbf{H_2GL^1}$ ([$\mathbf{H_2GL^1}$] = 0.13 mM, 25 °C, I = 0.16 M NaCl).

taacetylglucose to afford compound **4**. $BF_3{\cdot}OEt_2$ was used as the Lewis acid promoter, and the yield of **4** was almost identical to a literature report of the same coupling using *p*-toluenesulfonic acid under Helferich conditions.[42] Glycosylation occurred exclusively at the less hindered alcohol in 72% overall yield (97% β and 3% α). The β anomer was then coupled with *N*,*N*′-dimethylethylenediamine via a Mannich condensation, and the acetyl groups were removed to afford $\mathbf{H_2GL^2}$.

An ellipsoid plot of $\mathbf{H_2GL^2}$ is shown in Figure 1 with selected bond lengths and intramolecular H-bonding interactions presented in Table 2. The carbohydrate moieties participate in a network of intermolecular hydrogen-bonding interactions in the solid state, accounting for the observed packing arrangement in the crystal. Intramolecular H-bonding interactions between the amine nitrogen atoms and the H atoms of the hydroxyl groups are evident (shown by dashed lines in Figure 1). These H bonds were determined to have an important stabilizing effect in solution for the neutral $\mathbf{H_2GL^1}$ and $\mathbf{H_2GL^2}$ species (vide infra).

Both $\mathbf{H_2GL^1}$ and $\mathbf{H_2GL^2}$ were investigated by potentiometry to determine the ability of these compounds to compete with biological ligands (notably Aβ) for excess Cu and Zn. Potentiometric titrations of these two ligands were first completed to determine the acidity constants ($K_{a1}-K_{a4}$) of these compounds (Table 3); the results were then used as constants in the Zn and Cu metal binding studies.

Due to the limitations of potentiometry (inaccurate due to ionic strength changes when pH < 2.5 or > 11), UV−vis spectrophotometry was used to determine pK_a values outside the usable pH range of potentiometry. In addition, as potentiometry does not provide microscopic information involving identification of protonation sites on the ligands, spectroscopic methods (UV−vis/^{1}H NMR) were used to assign pK_a values to ionizable sites on the ligands. There are four ionizable groups of interest on $\mathbf{H_2GL^1}$ or $\mathbf{H_2GL^2}$: two tertiary amines and two phenol moieties as it is unlikely that deprotonation of the OH groups of glucose occurs in the pH range examined in this work.[64,65]

For $\mathbf{H_2GL^1}$, three acidity constants (pK_{a1}, pK_{a2}, and pK_{a3}) could be accurately determined by potentiometry while two acidity constants (pK_{a3} and pK_{a4}) could be evaluated spectrophotometrically. The values for pK_{a3} determined by the two methods (pK_{a3} = 10.2(2) via UV−vis; pK_{a3} = 10.30(5) via potentiometry) were found to agree very well. The first two acidity constants (pK_{a1}, pK_{a2}) for $\mathbf{H_2GL^1}$ were assigned to the tertiary amine moieties on the basis of variable pD ^{1}H NMR (data not shown) and pH UV−vis studies (Figure 2). The pH UV−vis experiment exhibited a bathochromic shift of the aromatic $\pi \rightarrow \pi^*$ transition (and an increase in ϵ_{max}) due to deprotonation of the two phenol moieties in the basic pH region.[66]

The order of deprotonation for the ammonium and phenol moieties in $\mathbf{H_2GL^1}$ parallels that for related aminophenol compounds.[39,67,68] The weak basicity of the ammonium moieties is most probably due to the stability afforded by formation of intramolecular hydrogen bonds (6-membered rings) between the amine nitrogen atoms and the H atoms of the hydroxyl groups for the neutral species $\mathbf{H_2GL^1}$. H bonding thus weakens the proton affinity of the amino groups, increasing the stability of the phenol O−H bond.[39,68,69] This same H-bonding pattern is evident in the X-ray structure (Figure 1) of $\mathbf{H_2GL^2}$.

The acidity constants for $\mathbf{H_2GL^2}$ were determined and assigned in much the same way as for $\mathbf{H_2GL^1}$. Due to the increased basicity of the phenolic moieties of $\mathbf{H_2GL^2}$, both pK_{a3} and pK_{a4} were determined spectrophotometrically (see Supporting Information). Simulation of the spectrophotometric titration

(64) Nielsen, H.; Sorensen, P. E. *Acta Chem. Scand. A* **1983**, *37*, 105. (b) Ballinger, P.; Long, F. A. *J. Am. Chem. Soc.* **1960**, *82*, 795.
(65) Kapinos, L. E.; Song, B.; Sigel, H. *Chem. Eur. J.* **1999**, *5*, 1794.
(66) Silverstein, R. M.; Bassler, G. C.; Morrill, T. C. *Spectrometric Identification of Organic Compounds*, 4th ed.; Wiley: New York, 1981.
(67) Wong, E.; Caravan, P.; Liu, S.; Rettig, S. J.; Orvig, C. *Inorg. Chem.* **1996**, *35*, 715.
(68) L'Eplattenier, R.; Murase, I.; Martell, A. E. *J. Am. Chem. Soc.* **1967**, *89*, 837.
(69) Freedman, H. H. *J. Am. Chem. Soc.* **1961**, *83*, 2900.

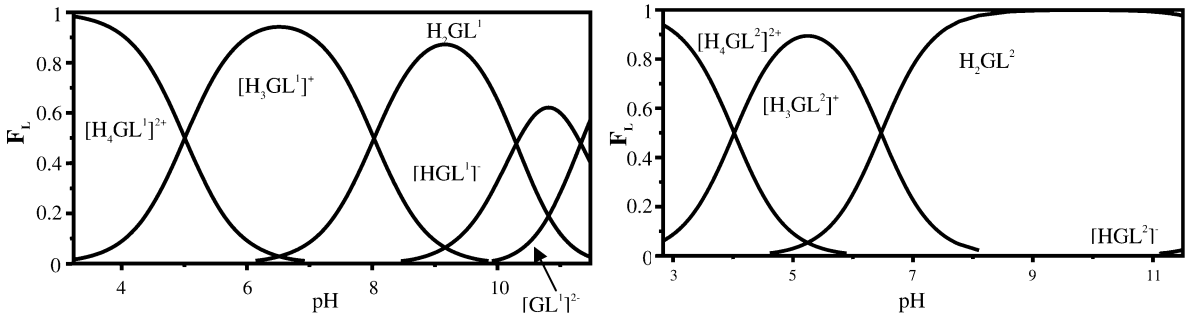

Figure 3. Solution speciation diagrams for $\mathbf{H_2GL^1}$ (0.6 M) and $\mathbf{H_2GL^2}$ (0.6 M); F_L = fraction of compound with given protonation.

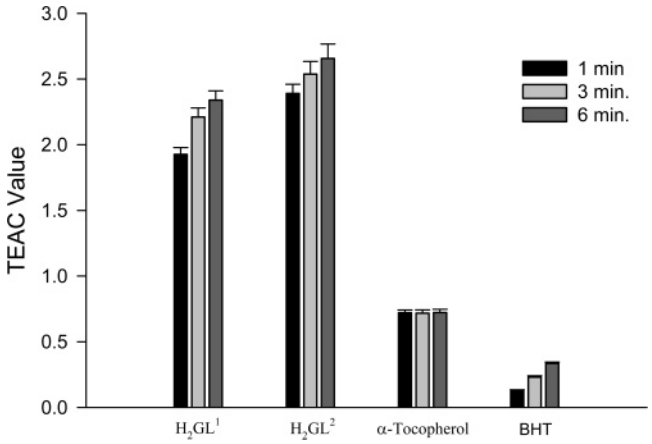

Figure 4. Trolox equivalent antioxidant capacity (TEAC) values at 1, 3, and 6 min for $\mathbf{H_2GL^{1,2}}$, (±)-α-tocopherol, and BHT. Error bars represent ±SD above and below the average TEAC value (determined in triplicate).

data for $\mathbf{H_2GL^2}$ afforded only one pK_a with a value of 13.4(3). The calculated value most likely corresponds to an average of pK_{a3} and pK_{a4} as the two phenols are equivalent, and thus, the acidity constants should be similar. Statistical effects can be used to separate pK_{a3} and pK_{a4} from the single measured value.[55] For deprotonation of the first phenol there are two positions that can be deprotonated but only one position that can be protonated. This requires the measured acidity constant to be twice as acidic. For the second deprotonation step the reverse situation exists. Considering this statistical effect, the two acidity constants should differ by a factor of 4, and the values for pK_{a3} and pK_{a4} can be calculated according to eqs 1 and 2 (Table 3)

$$pK_{a3} = (pK_{a3} + pK_{a4})/2 - 0.3 \quad (1)$$

$$pK_{a4} = (pK_{a3} + pK_{a4})/2 + 0.3 \quad (2)$$

Using the acidity constants determined for $\mathbf{H_2GL^{1,2}}$, solution speciation diagrams were calculated and are shown in Figure 3. Due to the differences in the basicities of the phenolic moieties the neutral species $\mathbf{H_2GL^2}$ exists over a much larger pH range as compared to $\mathbf{H_2GL^1}$. Indeed, while $\mathbf{H_2GL^2}$ is the predominant species above pH 7, $[\mathbf{H_3GL^1}]^+$, $\mathbf{H_2GL^1}$, $[\mathbf{HGL^1}]^-$, and $[\mathbf{GL^1}]^{2-}$ exist in the solution speciation diagram for $\mathbf{H_2GL^1}$.

Antioxidant Activity of $\mathbf{H_2GL^{1,2}}$. $\mathbf{H_2GL^{1,2}}$ were monitored for antioxidant activity by the TEAC assay, which has been used to quantify the antioxidant activity of biological fluids, extracts, and pure compounds by measuring the disappearance of the $ABTS^{\bullet+}$ radical cation via UV−vis spectroscopy.[61] The ability of $\mathbf{H_2GL^{1,2}}$ to quench the $ABTS^{\bullet+}$ radical cation was compared to Trolox, a more water-soluble analog of α-tocopherol, and the results are shown in Figure 4. Both $\mathbf{H_2GL^{1,2}}$ exhibited TEAC values that were enhanced in comparison to (±)-α-tocopherol and butylated hydroxytoluene (BHT); however, it should be noted that each pro-ligand contains two phenolic moieties capable of quenching the $ABTS^{\bullet+}$ radical cation. $\mathbf{H_2GL^{1,2}}$ are essentially protected hydroquinones, and oxidation to the associated quinones could be the reason for the potent antioxidant properties. The increased activity of $\mathbf{H_2GL^2}$, as compared to the hydrogen analog $\mathbf{H_2GL^1}$, is most likely due to the increased stabilization of the phenoxy radical through inductive and/or steric effects from the *tert*-butyl group ortho to the ring hydroxyl.[43] It is clear from this study that $\mathbf{H_2GL^{1,2}}$ have the capability to act as antioxidant compounds contributing to the multifunctional nature of these potential AD therapeutics. Generation of ROS from reaction of the Cu complexes of $\mathbf{H_2GL^{1,2}}$ (vide infra) with dioxygen in vivo is a possibility which has not been explored in this work.

Ni^{2+} and Cu^{2+} Metal Complexes of $[\mathbf{GL^{1,2}}]^{2-}$. The neutral Ni^{2+} and Cu^{2+} complexes of $[\mathbf{GL^{1,2}}]^{2-}$ were synthesized in MeOH with the addition of base. The Cu complexes were characterized by MS, EA, UV−vis, EPR, and μ_{eff}, while the Ni complexes were characterized by MS and EA. The Cu and Ni complexes of $[\mathbf{GL^{1,2}}]^{2-}$ were further characterized by X-ray crystallography. The green Cu complexes exhibited characteristic $[Cu + Na]^+$ and/or $[Cu + H]^+$ ion peaks with the correct isotope patterns by +ES-MS. Elemental analysis of the bulk samples correlated well for $\mathbf{CuGL^1}\cdot 2H_2O$ and $\mathbf{CuGL^2}\cdot 2MeOH$, respectively. The different associated solvents (H_2O vs MeOH) are a result of the purification procedure used, and these could not be removed upon prolonged drying. It is assumed that due to Jahn−Teller distortion, there is a weak axial interaction between the residual solvents and the square-planar Cu centers. The red/brown Ni complexes exhibited characteristic $[Ni + Na]^+$ and/or $[Ni + H]^+$ ion peaks by +ES-MS. Elemental analysis of the bulk samples correlated well for $\mathbf{NiGL^1}\cdot 3H_2O$ and $\mathbf{NiGL^2}\cdot H_2O$, respectively. Ni complexes with N-glycoside ligands have been shown to exhibit antifungal activity.[70] The experimental magnetic moments for $\mathbf{CuGL^1}$ (1.74 BM) and $\mathbf{CuGL^2}$ (1.79 BM) were found to be very close to the spin-only value (1.73 BM) at room temperature. Frozen solution (T = 130 K) X-band EPR spectra for the two Cu complexes were recorded, and appropriate spin Hamiltonian parameters were derived from simulation of the experimental spectra. As expected, both $\mathbf{CuGL^1}$ and $\mathbf{CuGL^2}$ exhibited patterns typical for tetragonal Cu(II)−N_2O_2 centers (see Supporting Information).[71]

(70) Yano, S.; Inoue, S.; Nouchi, R.; Mogami, K.; Shinohara, Y.; Yasuda, Y.; Kato, M.; Tanase, T.; Kakuchi, T.; Mikata, Y.; Suzuki, T.; Yamamoto, Y. *J. Inorg. Biochem.* **1998**, *69*, 15.

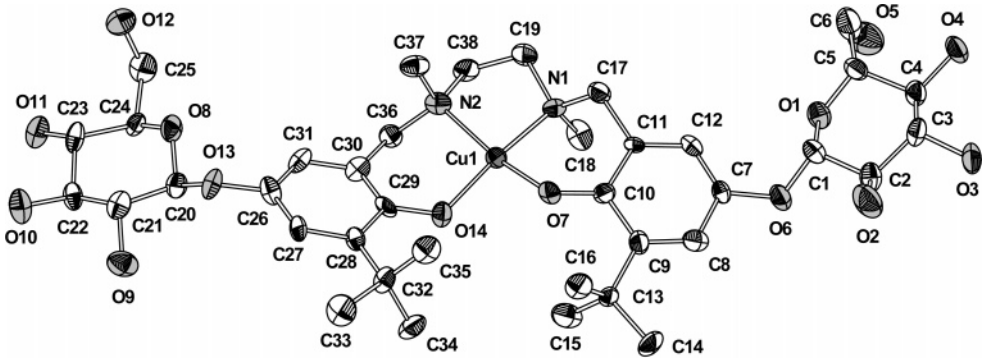

Figure 5. Ellipsoid plot (50% probability, H atoms omitted for clarity) of **CuGL²**.

Table 4. Selected Bond Lengths (Å) and Angles (deg) in **CuGL²** and **NiGL²**

	M = Cu	M = Ni		M = Cu	M = Ni
M(1)−N(1)	2.002(6)	1.90(1)	N(1)−M(1)−N(2)	86.4(3)	87.8(4)
M(1)−N(2)	2.042(7)	1.942(9)	N(1)−M(1)−O(7)	92.7(2)	94.2(4)
M(1)−O(7)	1.893(5)	1.907(8)	N(2)−M(1)−O(14)	93.2(2)	92.6(4)
M(1)−O(14)	1.906(5)	1.838(8)	O(7)−M(1)−O(14)	92.2(2)	87.0(3)
C(7)−O(6)	1.430(8)	1.42(1)	M(1)−N(1)−C(17)	112.1(4)	113.9(8)
C(1)−O(6)	1.415(8)	1.40(1)	M(1)−N(2)−C(36)	109.4(5)	111.2(8)
C(20)−O(13)	1.381(8)	1.42(1)	O(6)−C(1)−O(1)	106.7(6)	105(1)
C(1)−O(1)	1.449(8)	1.42(1)	O(13)−C(20)−O(8)	106.5(5)	105.9(9)
C(10)−O(7)	1.307(9)	1.38(1)			
C(29)−O(14)	1.343(9)	1.32(1)			
C(17)−N(1)	1.470(9)	1.51(1)			
C(36)−N(2)	1.499(9)	1.47(2)			
C(19)−C(38)	1.53(1)	1.51(2)			

Table 5. Stability Constants of the Cu^{2+} and Zn^{2+} Complexes with $H_2GL^{1,2}$ Determined by Potentiometric Measurement in 0.16 M NaCl at 298 K

	log *K*			
	H_2GL^1		H_2GL^2	
	Zn^{2+}	Cu^{2+}	Zn^{2+}	Cu^{2+}
$M^{2+} + \mathbf{H_2GL^{1,2}} \leftrightarrows [\mathbf{MH_2GL^{1,2}}]^{2+}$		7.23(5)		5.75(8)
$M^{2+} + [\mathbf{HGL^{1,2}}]^{+} \leftrightarrows [\mathbf{MHGL^{1,2}}]^{+}$	7.8(2)	14.05(6)	9.3(2)	14.83(5)
$M^{2+} + [\mathbf{GL^{1,2}}]^{2-} \leftrightarrows \mathbf{MGL^{1,2}}$	12.90(8)	20.46(4)	16.83(5)	24.18(2)
$\mathbf{MGL^{1,2}} + H_2O \leftrightarrows [\mathbf{MGL^{1,2}}(OH)]^{-} + H^{+}$	−11.0(6)	−11.1(4)	−11.1(4)	−10.9(3)

There are a significant number of Cu and Ni complexes containing carbohydrate-derived ligands reported in the literature;[72−74] in almost all cases, however, the carbohydrate moiety is bound to the metal center. Only two X-ray structures of Ni and Cu complexes containing pendant carbohydrate ligands exist: a Ni complex of a 1,3-diaminosugar[73] and a Cu complex with xylose-appended serine ligands.[74] Importantly, the carbohydrate moieties remain pendant in both the Ni and Cu complexes of **H₂GL²**. The structure of **CuGL²** is shown in Figure 5 with selected bond lengths and angles for the Cu and Ni derivatives presented in Table 4. **CuGL²** possesses a distorted square-planar geometry; the dihedral angle between the least-squares planes through Cu(1)N(1)O(7) and Cu(1)N(2)O(14) is 22.1°.

CuGL² crystallized with two molecules in the asymmetric unit, one of each diastereomer. The carbohydrate moieties participate in a network of hydrogen-bonding interactions, both between and along the sheets, accounting for the packing arrangement in the crystal. Removal of the solvent molecules in the structure solution precluded the observation of H-bonding interactions mediated by the solvent molecules. The structure of the Ni complex was very similar to that for Cu and is included in the Supporting Information. Complexation of the pro-ligands **H₂GL^{1,2}** with Zn was only partially successful on the macroscopic scale. Evidence for complexation via +ES-MS ($[Zn + Na]^+$ and/or $[Zn + H]^+$) was encouraging, yet the complexes could not be purified satisfactorily.

The solution speciation of Cu^{2+} and Zn^{2+} with **H₂GL^{1,2}** was studied by potentiometric titrations. The pK_a values for the ligands as well as the hydrolysis reactions of free Cu^{2+} and Zn^{2+} were included as constants in the calculations.[60] The values in Table 5 show that **H₂GL²** exhibits larger binding constants (log $K_{\mathbf{MGL^{1,2}}}$) with Zn^{2+} and Cu^{2+} than does **H₂GL¹**.

This result is expected as binding constants for a particular metal ion should increase with increasing ligand basicity for a series of similar ligands.[65,75,76] On the basis of the calculated constants, solution speciation diagrams were calculated for Zn^{2+} and Cu^{2+} with **H₂GL¹** and **H₂GL²** (Figure 6). Except for the presence of $[\mathbf{CuH_2GL^{1,2}}]^{2+}$ in the Cu^{2+} systems, the species present in the pH range examined are identical for both Zn^{2+} and Cu^{2+}. From the speciation diagrams it is obvious that no free Cu^{2+} exists above pH 5 with either ligand, while free Zn^{2+} exists up to pH 7. Due to the higher stability of the **CuGL^{1,2}** species as compared to **ZnGL^{1,2}**, the former species are more predominant at lower pH and exist over a larger pH range. Indeed, at pH 7, **CuGL^{1,2}** is the sole species present for Cu^{2+}, while **ZnGL^{1,2}**, Zn^{2+}, and $[\mathbf{ZnHGL^{1,2}}]^+$ exist for the Zn^{2+} systems. No metal hydrolysis species of significance were present in any of the systems studied.

Comparison of the calculated Cu^{2+} and Zn^{2+} stability constants of **H₂GL^{1,2}** with relevant chelators is of significant interest. However, while stability constants are a measure of the overall stability of a metal−ligand species, they do not reflect the metal-binding affinity of ligands at a specific pH value, and thus a direct comparison can be misleading. For a given complex equilibrium system and pH the concentration of unchelated metal ion (referred to as $pM = -\log[M_{unchelated}]$) represents a direct

(71) Peisach, J.; Blumberg, W. E. *Arch. Biochem. Biophys.* **1974**, *165*, 691.
(72) (a) Tanase, T.; Kurihara, K.; Yano, S.; Kobayashi, K.; Sakurai, T.; Yoshikawa, S.; Hidai, M. *Inorg. Chem.* **1987**, *26*, 3134. (b) Tanase, T.; Yasuda, Y.; Onaka, T.; Yano, S. *Dalton Trans.* **1998**, 345. (c) Tanase, T.; Inukai, H.; Onaka, T.; Kato, M.; Yano, S.; Lippard, S. J. *Inorg. Chem.* **2001**, *40*, 3943. (d) Tanase, T.; Doi, M.; Nouchi, R.; Kato, M.; Sato, Y.; Ishida, K.; Kobayashi, K.; Sakurai, T.; Yamamoto, Y.; Yano, S. *Inorg. Chem.* **1996**, *35*, 4848. (e) Mikata, Y.; Sugai, Y.; Yano, S. *Inorg. Chem.* **2004**, *43*, 4778.
(73) Yano, S. et al. *Chem. Lett.* **1999**, 255.
(74) Delbaere, L. T. J.; Kamenar, B.; Prout, K. *Acta. Crystallogr., Sect. B* **1975**, *31*, 862.
(75) Chiu, Y.; Canary, J. W. *Inorg. Chem.* **2003**, *42*, 5107.
(76) Martin, R. B.; Sigel, H. *Comments Inorg. Chem.* **1988**, *6*, 285.

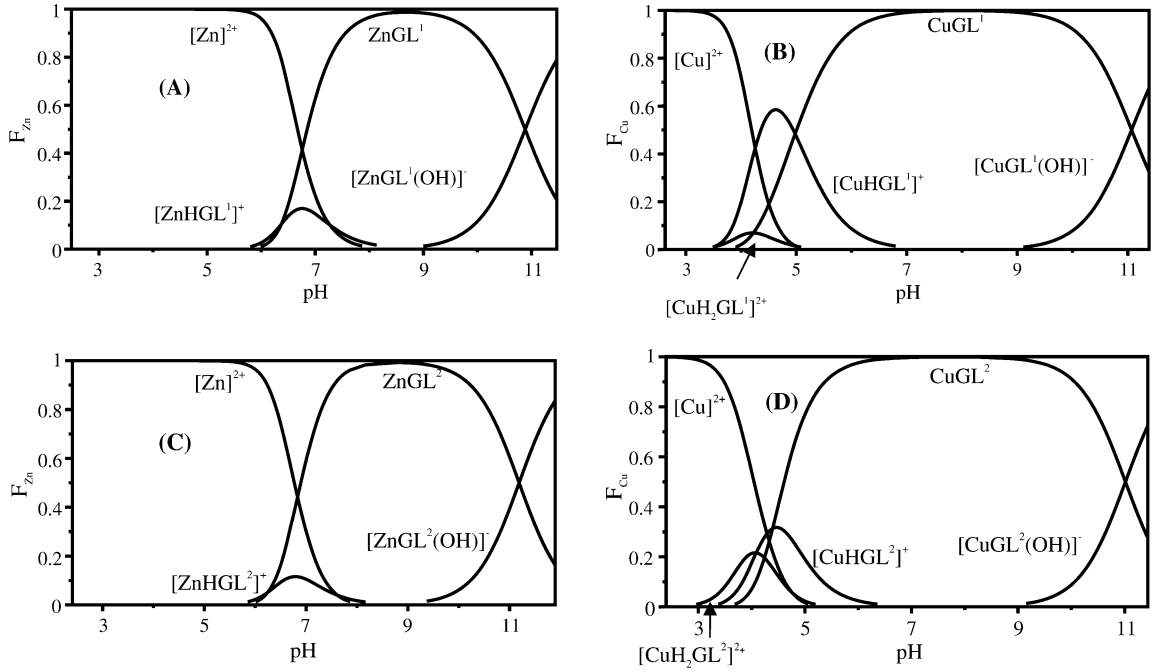

Figure 6. Solution speciation diagrams for (A) $\mathbf{H_2GL^1}$ and Zn^{2+}, (B) $\mathbf{H_2GL^1}$ and Cu^{2+}, (C) $\mathbf{H_2GL^2}$ and Zn^{2+}, and (D) $\mathbf{H_2GL^2}$ and Cu^{2+} ([$\mathbf{H_2GL^{1,2}}$]:[M^{2+}], 1.1:1; [M^{2+}] = 0.6 mM).

Table 6. Calculated pM ($-\log[M]_{unchelated}$; M = Zn^{2+}, Cu^{2+}) for a Solution Containing a 1:1 Mixture of Indicated Compound and Metal Ion ($[M^{2+}]_{tot}$ = [chelator]$_{tot}$ = 0.001 M)

	pZn	pCu	
compound	pH 7.4	pH 6.6	pH 7.4
H_2GL^1	4.2	6.8	7.9
H_2GL^2	3.9	6.6	7.5
DTPA	8.4[a]	9.3[a]	10.1[a]

[a] Values calculated from ref 40.

estimate of the ligand−metal affinity taking into account all relevant equilibria.[75,77] pM depends on ligand and metal concentration, temperature, ionic strength, and pH of the solution. Table 6 shows the calculated pM values (pH 7.4) for solutions containing 1 mM of metal (M = Zn^{2+} or Cu^{2+}) and 1 mM of either $\mathbf{H_2GL^1}$, $\mathbf{H_2GL^2}$, or DTPA. In addition, pCu values were calculated at lower pH (pH 6.6) where Cu-induced aggregation of Aβ is accelerated.[10] Interestingly, although $\mathbf{H_2GL^2}$ has larger zinc and copper binding constants compared to those of $\mathbf{H_2GL^1}$, the affinity of $\mathbf{H_2GL^2}$ for these metals is lower at pH 6.6 and 7.4 due to the greater proton affinity of $\mathbf{H_2GL^2}$. At physiological pH (pH = 7.4) the pZn values for $\mathbf{H_2GL^1}$ (pZn = 4.2) and $\mathbf{H_2GL^2}$ (pZn = 3.9) are quite similar yet substantially lower than that for DTPA (pZn = 8.4). Again, the pZn values can be attributed to the difference in proton affinity of $\mathbf{H_2GL^{1,2}}$ compared with that of DTPA. Much the same trend exists for copper; the related pCu values (at either pH 6.6 or 7.4) are lower for $\mathbf{H_2GL^{1,2}}$ compared with DTPA (Table 6). The pCu values for $\mathbf{H_2GL^{1,2}}$ correspond to approximate dissociation constants (K_d) in the nanomolar range, slightly lower than those reported (0.1−5 μM) in Cu−Aβ peptide binding studies.[10,78,79] The substantially lower K_d value (attomolar) for the Cu−Aβ_{1-42} complex described by Atwood et al.[80] is most likely a result of rapid peptide aggregation (under kinetic control) during the competitive metal capture assay. The pZn values for $\mathbf{H_2GL^{1,2}}$ correspond to approximate K_d values in the micromolar range, comparable to reported values (2−300 μM) for Zn binding to the Aβ peptide.[78,81] Thus, the affinities of $\mathbf{H_2GL^{1,2}}$ for Zn and Cu at physiological pH suggest that the chelators will compete with all soluble forms of Aβ for these metal ions (vide infra).

Aβ Aggregation Inhibition Studies. The ability of $\mathbf{H_2GL^{1,2}}$ to inhibit metal-ion-induced Aβ-peptide aggregation was assessed via a turbidometry assay. It has been shown previously that metal ions such as Zn^{2+} and Cu^{2+} promote the rapid aggregation of Aβ and that metal chelators can attenuate these effects.[9,10,28,82] Similarly, in this study both $\mathbf{H_2GL^{1,2}}$ were shown to reduce Zn^{2+}-induced Aβ_{1-40} aggregation by approximately 50% at physiological pH (Figure 7). The strong metal-ion chelator DTPA was, as expected, even more effective at reducing Zn^{2+}-induced aggregation of the Aβ peptide. The slightly enhanced activity of $\mathbf{H_2GL^1}$ over $\mathbf{H_2GL^2}$ can be attributed to the increased metal-binding affinity of the former at physiological pH. The effect of these ligands on Cu^{2+}-induced Aβ_{1-40} aggregation was also assessed but at a lower pH (pH 6.6). The interaction of the Aβ peptide with Cu^{2+} is known to be pH dependent[10] with no aggregation apparent at physiological pH (data not shown). At this lower pH Cu^{2+}-induced Aβ_{1-40}

(77) (a) Fahrni, C. J.; O'Halloran, T. V. *J. Am. Chem. Soc.* **1999**, *121*, 11448. (b) Martell, A. E.; Hancock, R. D. *Metal Complexes in Aqueous Solutions*; Plenum Press: New York, 1996.

(78) Garzon-Rodriguez, W.; Yatsimirsky, A. K.; Glabe, C. G. *Bioorg. Med. Chem. Lett.* **1999**, *9*, 2243. (a) Danielsson, J.; Pierattelli, R.; Banci, L.; Graslund, A. *FEBS Lett.* **2007**, *274*, 46.

(79) (a) Hou, L. M.; Zagorski, M. G. *J. Am. Chem. Soc.* **2006**, *128*, 9260. (b) Syme, C. D.; Nadal, R. C.; Rigby, S. E. J.; Viles, J. H. *J. Biol. Chem.* **2004**, *279*, 18169. (c) Guilloreau, L.; Damian, L.; Coppel, Y.; Mazarguil, H.; Winterhalter, M.; Faller, P. *J. Biol. Inorg. Chem.* **2006**, *11*, 1024. (d) Kowalik-Jankowska, T.; Ruta, M.; Wisniewska, K.; Lankiewicz, L. *J. Inorg. Biochem.* **2003**, *95*, 270.

(80) Atwood, C. S.; Scarpa, R. C.; Huang, X.; Moir, R. D.; Jones, W. D.; Fairlie, D. P.; Tanzi, R. E.; Bush, A. I. *J. Neurochem.* **2000**, *75*, 1219.

(81) (a) Clements, A.; Allsop, D.; Walsh, D. M.; Williams, C. H. *J. Neurochem.* **1996**, *66*, 740. (b) Bush, A. I.; Pettingell, W. H., Jr.; Paradis, M. d.; Tanzi, R. E. *J. Biol. Chem.* **1994**, *269*, 12152.

(82) Huang, X. D.; Atwood, C. S.; Moir, R. D.; Hartshorn, M. A.; Vonsattel, J. P.; Tanzi, R. E.; Bush, A. I. *J. Biol. Chem.* **1997**, *272*, 26464.

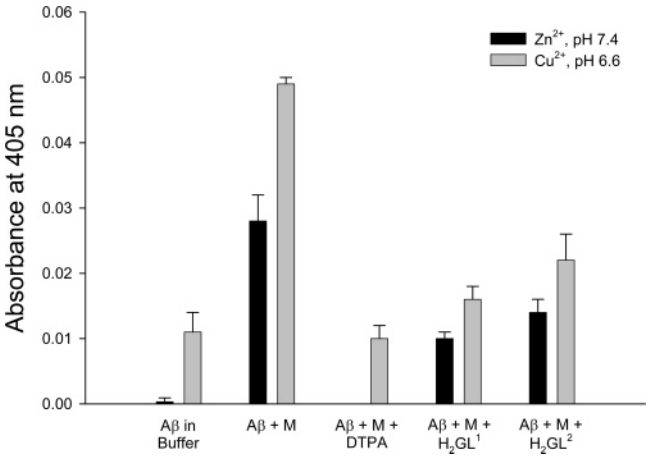

Figure 7. Aggregation inhibition assay of Aβ_{1-40}. Data indicate the mean absorbance (at least three trials) at 405 nm of Aβ solutions in buffer: in the absence of metal ion (M), in the presence of M (Zn^{2+} at pH 7.4 or Cu^{2+} at pH 6.6), and in the presence of M and test ligand (DTPA, **H_2GL^1**, or **H_2GL^2**). Error bars represent $\pm$SD above (and below, not shown) the average absorbance value.

aggregation was significantly attenuated with both **$H_2GL^{1,2}$** as well as DTPA (Figure 7). We cannot rule out that both **$H_2GL^{1,2}$**, or their respective Zn or Cu complexes, inhibit peptide aggregation at least partially through intercalation.[27,83]

Summary. In this work we have shown that the water-soluble, carbohydrate-containing compounds **$H_2GL^{1,2}$** have significant antioxidant capacity on the basis of an in vitro antioxidant assay. In addition, the two compounds have a moderate affinity for Cu^{2+} and Zn^{2+} and decrease Aβ_{1-40} aggregation induced by these metal ions. **$H_2GL^{1,2}$** may be ideally suited for disruption of the abnormal metal−protein interactions in the brain possibly responsible for the observed toxicity in AD. The moderate affinity of **$H_2GL^{1,2}$** for metal ions at physiological pH may obviate the toxicity commonly associated with chelation therapy, especially when coupled with the potential for increased tissue specificity due to the attached carbohydrate functions. In addition, the phenolic moieties of the apo-chelators can act as antioxidants, contributing to the multifunctional nature of these potential Alzheimer's disease therapeutics.

Acknowledgment. The authors gratefully acknowledge the Canadian Institutes of Health Research (CIHR) for a Proof of Principle grant. T.S. acknowledges NSERC for a postgraduate scholarship, L.E.S. recognizes support from the Alzheimer's Society of Canada for a training award, and M.M. acknowledges the Alexander von Humboldt Foundation for a Feodor Lynen postdoctoral fellowship. Dr. Bin Song is thanked for help with the potentiometric analysis. Dr. Wilf Jeffries is acknowledged for generous donation of a sample of Aβ_{1-40} peptide.

Supporting Information Available: Complete refs 13, 15b, 20, 23b, and 73, variable pH UV−vis titration data for **H_2GL^2**, the ellipsoid plot of **$NiGL^2$**, as well as EPR spectra and simulations of **$CuGL^1$** and **$CuGL^2$**; X-ray crystallographic files in CIF format of **H_2GL^2**, **$CuGL^2$**, and **$NiGL^2$**. This material is available free of charge via the Internet at http://pubs.acs.org.

JA068965R

(83) Raman, B.; Ban, T.; Yamaguchi, K.; Sakai, M.; Kawai, T.; Naiki, H.; Goto, Y.; *J. Biol. Chem.* **2005**, *280*, 16157.